

Determining isotopy classes of crossing arcs in alternating links

Anastasiia Tsvietkova

Abstract. For a reduced alternating diagram, we obtain the conditions that guarantee that the link complement has the complete hyperbolic structure, and every intercusp crossing arc is an edge of an ideal geometric partially flat triangulation and is isotopic to a simple geodesic. We provide a examples of links for which this holds, including infinite families of closed alternating braids.

Key words and phrases: alternating link, link complement, hyperbolic structure, geodesic

MSC 2010: 57M25, 57M50

1 Overview

A link diagram provides a combinatorial description of a topological object, a link complement in S^3 . A natural question arising from this description is whether the complement can be endowed with a complete hyperbolic structure, which is unique in the view of Mostow-Prasad rigidity ([9, 10]).

This question is connected with the question of the existence of an ideal geometric triangulation of the complement. By an ideal triangulation we mean a collection of 3-simplices with vertices deleted. In place of these vertices, there are cross-sectional triangles. By “geometric”, a properly embedded triangulation that agrees with the complete hyperbolic structure of the 3-manifold is meant, if such a structure exists.

While both of these questions can often be answered after tedious computations for a particular link, it is not *a priori* clear what would be a successful choice of edges for such a triangulation.

In this note, we show that under certain conditions that can be checked from the link diagram, the crossing arcs of a reduced alternating diagram are the edges we need. By crossing arcs we mean an intercusp arc traveling from the underpass to the overpass of a crossing. The triangulation obtained is geometric, and induces the complete hyperbolic metric on the link complement. This allows us to prove that under these conditions, crossing arcs are isotopic to geodesics.

This observation has a long history. W. Thurston noticed that if we choose a decomposition of a hyperbolic link complement in two polyhedra where edges are crossing arcs of a link diagram, then we often obtain an ideal geometric triangulation from it (by subdivision) ([14]). The method was generalized by Menasco for alternating links ([7]), and by Petronio beyond alternating ([11]). While this suggests that the arcs are often isotopic to geodesics, the procedure fails to provide a geometric triangulation in general. On the other hand, Sakuma and Weeks conjectured that crossing arcs of a reduced alternating diagram are the arcs of the canonical cell decomposition of the link complement ([13]), which would imply they are isotopic to geodesics as well. However, the conjecture is far from being proved.

Overall, there are only a few results that identify arcs with a certain topological or combinatorial description as geodesics. Miller investigated isotopy classes of closed geodesics ([8]). As for intercusp arcs, the only results known to the author are either the examples of canonical cell decompositions by Sakuma and Weeks that imply that crossing arcs of some families of symmetric alternating links are isotopic to geodesics (see Examples I.2.2-I.2.4 in [13]), or work done by Adams, Burton, Cooper, Futer, Purcell, and Reid that provides information about isotopy classes of certain tunnel arcs under additional restrictions ([1, 2, 3, 4]).

The sufficient conditions we obtained turn out to have a simple geometric meaning. Let us return again to the polyhedral decomposition suggested by Thurston and described by Menasco for alternating links. The term “polyhedron” is used only in topological sense here, since even for a hyperbolic link the faces might not be planar, *i.e.* might not lie in one hyperbolic plane. We will call such a polyhedron *cross-sectionally convex*, if at every ideal vertex all interior angles of a cross-section are in $(0, \pi)$. Note that this is not equivalent to the usual convexity: the faces might still be non-planar and, when subdivided, might yield a non-convex polyhedron.

The conditions that we obtain imply cross-sectional convexity of two polyhedra suggested by Thurston. Then we show that every cross-sectionally convex polyhedral decomposition can be subdivided into ideal geometric partially flat triangulation (“partially flat” means some tetrahedra have 0 volume, while the rest have positive volume). In particular, the purely combinatorial algorithm described by Menasco for alternating links then provides an ideal geometric partially flat triangulation.

The existence of an ideal partially flat geometric triangulation is a necessary and sufficient condition for the existence of the complete hyperbolic structure on a 3-manifold ([12]). Such triangulations appear to be useful for various other purposes as well (see, for example, [6]).

The following is a short overview of our methods and techniques. In [15], an alternative way of parameterizing hyperbolic structures of links is introduced. In particular, it uses complex labels assigned to a link diagram that describe horoball structures in \mathbb{H}^3 . We will refer to these labels as to diagram labels. The triangulation is not performed, and instead the method uses isometries of preimages of polygons bounded by the regions of the link diagram. This results in a set of relations, to which we will refer as to hyperbolicity relations.

The authors of [15] start with a hyperbolic link, and then describe the relations for the diagram labels merely as a convenient method for computing the (already existent) complete hyperbolic structure of the complement. Here, we rather start with an arbitrary link diagram and the complex labels that satisfy the hyperbolicity relations for this diagram, and then establish the conditions on the labels that guarantee the existence of the induced complete hyperbolic structure.

The paper is organized as follows. In Sections 2-3 we describe a setting in which we work, recalling the nature of the conditions that make an ideal triangulation geometric, and developing a model that would give the complete hyperbolic structure based on the diagram labels rather than a triangulation process. In Section 4, we lay out and explain the conditions on diagram labels sufficient for our purposes. In Section 5, we prove that under these conditions, the Thurston-Menasco’s polyhedral decomposition is properly embedded in H^3 . In Section 5, we show that, further, the decomposition yields an ideal partially flat geometric triangulation, and use this to make the conclusion about the complete hyperbolic structure of the link complement. Section 6 comments on crossing arcs being isotopic to simple geodesics under the conditions provided. It also provides examples (one of which is an infinite family of braids) demonstrating that one can check the conditions easily from a link diagram.

2 Diagram labels

Consider the complement of a link L in S^3 , and a diagram D of L . In what follows, we will describe the correspondence between the points on the peripheral boundary of $S^3 - L$ and the points in the boundary of \mathbb{H}^3 through a solution of the hyperbolicity equations, introduced in [15]. In further sections, we will investigate under which conditions on the labels this correspondence yields the complete hyperbolic structure and the developing map for the manifold $S^3 - L$.

Every region R of D that is incident to at least three crossings may be viewed as a disk bounded by the geodesic arcs traveling from the overpass to the underpass at every crossing of R , and by the arcs traveling on the boundary torus from one crossing of R to the next crossing of R (black and gray arcs on Fig.1, left, respectively, where a region incident to three crossings is depicted). Every arc can be assigned a complex number - a diagram label. When the complete hyperbolic structure exists on $S^3 - L$, the diagram labels are called crossing and edge labels respectively, and they parametrize the hyperbolic structure (see [15] for details and geometric definitions of the labels).

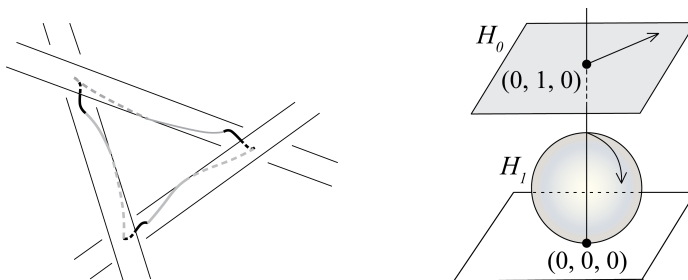


Fig.1

Hyperbolicity relations are two sets of polynomial relations in the diagram labels. The first set, called the region relations, guarantees that the composition of hyperbolic isometries rotating a preimage of the boundary of every described disk in \mathbb{H}^3 is an identity. If the region is 2-sided (*i.e.* it is a bigon), the two edge labels inside it are set to 0, and the two crossing labels are set equal, which corresponds to having no disk, but rather two homotopic geodesic arcs at crossings. The second set of relations (called the edge relations) for alternating links consists of relations of the form either $u = v \pm 1$ or $u = v$, where u, v are two edge labels assigned to two different sides of the same edge of D . They guarantee that whenever two arcs on the boundary torus form a simple closed curve going around a strand of L , the curve is homotopic to a meridian of the length 1. We refer the reader to [15] for further details and examples.

Assume that there is a complex solution \bar{x} to the hyperbolicity relations for D (it is possible that all entries of \bar{x} have 0 imaginary part, and therefore are real). In particular, if there are n crossings in D , \bar{x} consists of n crossing labels w_1, w_2, \dots, w_n , and $2n$ edge labels u_1, u_2, \dots, u_{2n} .

Locally, the boundary torus for every link component can be endowed with a Euclidean structure. At an overpass or an underpass of a crossing of D , choose a cross-section of the torus with a unit meridian. Let the cross-section correspond to an infinite union of Euclidean planes, and let the meridian correspond to the real number 1 on each of them. We will view each of these planes in the Euclidean three-dimensional space as a sphere minus the South pole, touching the plane $z = 0$ from above. We may consider these spheres as horospheres in the upper-half space, *i.e.* as hyperplanes in \mathbb{H}^3 (using the upper half-space model of \mathbb{H}^3).

In what follows, we will connect the points where the horospheres are tangent to the plane $z = 0$ (we call such a point P_i the center of the corresponding horosphere H_i) by hyperbolic geodesics. We will situate and scale the horospheres so that the geometric definitions of the diagram labels are satisfied, even though the link L might not be hyperbolic. For this, we use a correspondence between the points P_i on the boundary of \mathbb{H}^3 and the points \bar{P}_i on the boundary torus of $S^3 - L$. In particular, for each overpass or underpass of D we consider one point \bar{P}_i on the boundary torus, and a horosphere for which this is a point of tangency with \mathbb{H}^3 .

To specify the size and the exact location of the horospheres, consider a region R_0 of D that has at least three crossings (and hence R_0 is not a bigon). There are three underpasses and overpasses together for two consecutive crossings. Suppose these underpasses and overpasses correspond to a sequence of horospheres H_0, H_1, H_2 in \mathbb{H}^3 , and the centers of H_0, H_1 are connected by the hyperbolic geodesic γ_1 , while the centers of H_1, H_2 are connected by γ_2 . Denote the preimage of the meridian on the horosphere H_i by m_i throughout.

If the crossing label that corresponds to γ_1 is 0, then the centers of the horospheres H_0, H_1 coincide, γ_1 is null-homotopic, and we can proceed to the next horosphere. So let us assume that this crossing label is not 0.

Place one of the horospheres, H_0 , as an “infinite” horosphere, the plane $z = k$. Introduce the coordinates for \mathbb{H}^3 (*i.e.* for the Euclidean 3-dimensional space were we choose to work with the upper-half space) so that $k = 1$, and the preimage of m_0 is the unit vector going from $(0, 1, 0)$ to $(1, 1, 0)$. Place H_1 at the point $(0, 0, 0)$ (as on Fig.1, right, the horospheres are shaded). We may assume that P_0, P_1 are distinct, since otherwise $|w| = 0$ (which happens iff $w = 0$). Scale H_1 in \mathbb{H}^3 so that $|w_1|$ is the Euclidean diameter of H_1 . Additionally, rotate H_1 so that the angle by rotation between m_0 and m_1 is $\arg w - \pi$. The horospheres H_0, H_1 are now situated so that the geometric definition of the crossing label w_1 from [15] is satisfied.

The geodesic γ_2 is uniquely defined by one of its endpoints, P_1 , and the corresponding edge label u which tells where γ_2 pierces H_1 . This determines the position of the other endpoint P_2 of γ_2 . The diameter of H_2 and the direction of m_2 is defined by the next w_2 . Proceeding similarly from a horosphere to horosphere, region by region, we obtain a uniquely defined and scaled collection of horoballs with geodesics connecting them, the coordinate system on \mathbb{H}^3 and the Euclidean coordinates on each horosphere such that the preimage of every meridian corresponds to the real number 1.

Since the link L is not necessarily a hyperbolic link, the described process might lead to certain degeneracy. For example, the picture may consist of a single horosphere, if all the labels are 0. In the ‘next sections we will prove that this set-up together with a few additional conditions on the labels induce a complete hyperbolic metric on $S^3 - L$.

3 Completeness and consistency conditions for a triangulation

Thurston provided sufficient conditions for an ideal triangulation of a finite volume 3-manifold to be geometric, that can be expressed in gluing and completeness equations ([14]) together with a certain restriction on a solution. In particular, all the dihedral angles of an ideal hyperbolic tetrahedron can be parametrized by one complex number, z , which is often called the shape of the tetrahedron. A solution to the gluing and completeness equations provides shapes of all tetrahedra in a chosen triangulation. If there exists a solution such that the shape of every tetrahedron has a positive imaginary part, then the corresponding ideal triangulation is geometric, and the 3-manifold is hyperbolic. We will refer to such triangulations as to positively oriented

geometric.

This is not a criteria, since the condition that all shapes have positive imaginary part is not necessary for the triangulation to be geometric. For example, for a few manifolds, the program SnapPea ([16]) obtains a geometric triangulation that is not positively oriented. The criteria is given rather by an ideal partially flat geometric triangulation ([12]). That is the type of triangulation that we will use. This section comments on the nature of the condition an ideal triangulation needs to satisfy in order to be geometric and partially flat.

The following is the list of the conditions that we seek in an ideal triangulation:

- (i) in every ideal simplex, every edge has an associated interior dihedral angle in the range of $[0, \pi]$;
- (ii) in every ideal simplex, the opposite dihedral angles are equal, and the interior angles of every triangular cross-section sum to π ;
- (iii) 3-simplices can be glued along their faces resulting in $S^3 - L$, the sum of the dihedral angles around each edge e is 2π after the gluing, and for any tetrahedron glued at e , there is no translational monodromy along e ;
- (iv) the resulting metric is complete, *i.e.* cross-sectional triangles glued together at each ideal vertex must fit together to give a closed Euclidean surface.

By Theorem 1.1 from [12] these conditions guarantee that an ideal triangulation, where not all tetrahedra are flat, and where the faces are glued by isometries (note that any two ideal triangles are congruent) to form $S^3 - L$, induces the complete hyperbolic metric on $S^3 - L$.

Let us recall what is a shape of an ideal hyperbolic tetrahedron (sometimes also called tetrahedral parameter or modulus). Consider a Euclidean cross-section of the tetrahedron. Suppose that the (complex) translations corresponding to the sides of the cross-section are $u, v, -(u+v)$ (Fig.2). Any of $-\frac{v}{u}, \frac{u}{u+v}, \frac{u+v}{v}$ can be taken as a shape z of the tetrahedron, and their arguments correspond to the interior Euclidean angles of the cross-section, as well as to the interior dihedral angles of the tetrahedron.

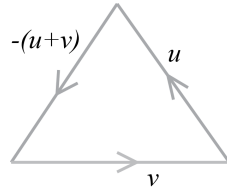


Fig.2

The condition (i) above is equivalent to $\text{Im } z \geq 0$. The condition (ii) is guaranteed if the pairs of opposite dihedral angles of the tetrahedron correspond to the arguments of $z, 1 - \frac{1}{z}, \frac{1}{1 - z}$. The condition (iii) holds if for every edge e of the triangulation, the shapes of k tetrahedra glued at e satisfy $z_1 z_2 \dots z_k = 1$ and $\arg z_1 + \arg z_2 + \dots + \arg z_k = 2\pi$ (not another multiple of 2π). However the next lemma shows that, if (iv) is satisfied, then condition $\arg z_1 + \arg z_2 + \dots + \arg z_k = 2\pi$ is actually redundant. The fact was known before, but, not being able to find it in exactly the same formulation in the literature, we provide a proof.

Lemma 3.1. Suppose k tetrahedra with the shapes z_1, z_2, \dots, z_k are glued at an edge e of a triangulation τ to obtain a cusped 3-manifold M . If $z_1 z_2 \dots z_k = 1$, and the completeness condition (iv) is satisfied. Then $\arg z_1 + \arg z_2 + \dots + \arg z_k = 2\pi$.

Proof. Let T be a boundary torus of M . There is a tiling Π of T by cross-sectional triangles that resulted from the gluing of tetrahedra of τ . Let F , E and V denote respectively the number of faces, edges and vertices in Π , and let F' , E' and V' be respectively the number of faces, edges and vertices of all cross-sectional triangles of τ (before the gluing).

Note that $V' = 3F' = 3F$, since the number of cross-sectional triangles is the same before and after the gluing, and each face has exactly three vertices. Note also that $V' = E' = 2E$, since each vertex in a cross-sectional triangle in τ corresponds to one edge of such triangle in τ , and, when glued, edges from E' are identified in pairs to obtain E . Therefore, $3F = 2E$.

The Euler characteristics for the torus is $\chi(M) = V - E + F = 0$. Together with the previous equality this gives $V - \frac{F}{2} = 0$.

Denote by A_v the sum of angles of the tiles of Π at a vertex v . If e is an edge of a tetrahedron in τ , and e is adjacent to v , then the angles that meet at v in Π correspond to the dihedral angles of tetrahedra in τ that meet at e under the gluing. By contradiction, suppose there is an edge e_0 of τ , incident to a vertex v_0 such that after the gluing is performed, $A_{v_0} > 2\pi$. Then the angle A_{v_0} determines a cone point on one of the cusp tori of the manifold. Without loss of generality, we may suppose this happens on T .

Since Π is a tiling by Euclidean triangles, the sum of interior angles of each its face is π . Therefore, if Δ_i , $i = 1, 2, \dots, n$, is the set of all triangular faces of Π , and α_i, β_i and δ_i are the interior angles of Δ_i , then

$$\begin{aligned} 0 &= \sum_{i=1}^n (\alpha_i + \beta_i + \delta_i - \pi) = \sum_{v \in V} A_v - \pi F = 2\pi V + \sum_{A_v > \pi} (A_v - 2\pi) - \pi F = \\ &= 2\pi(V - \frac{F}{2}) + \sum_{A_v > \pi} (A_v - 2\pi). \end{aligned}$$

Recall that we showed $V - \frac{F}{2} = 0$ above. Therefore, the above equality implies $\sum_{A_v > \pi} (A_v - 2\pi) = 0$.

However, by hypothesis, for every edge e the product of the corresponding shapes $z_1 z_2 \dots z_k = 1$, and hence each A_v in the latter sum (including A_{v_0}) is a nonnegative integer multiple of 2π . Such A_{v_0} cannot exist, a contradiction. \square

In the light of the lemma, we need to check that there exists an ideal triangulation τ , where faces can be identified to obtain $S^3 - L$, and the following holds:

- 1) in every tetrahedron, three pairs of opposite edges correspond to z , $1 - \frac{1}{z}$, $\frac{1}{1 - z}$ in the way indicated above;
- 2) at every edge e of τ , after all the faces are identified in pairs, the shapes of the tetrahedra glued at e satisfy $z_1 z_2 \dots z_k = 1$;
- 3) for every tetrahedron, its shape z satisfies $\text{Im } z \geq 0$;
- 4) the metric is complete, *i.e.* (iv) holds.

4 Decomposition into two properly embedded polyhedra

In this section, we consider a decomposition of the alternating link complement $S^3 - L$ into two ideal polyhedra, $\overline{\Pi}_1, \overline{\Pi}_2$, one above the reduced alternating diagram D of L , and one below, as described by Menasco in [7]. Assume additionally that the diagram D is twist reduced in the

sense of [5]. Every alternating link admits such a diagram (see Section 3 in [5] for the definition and explanation).

The polyhedra are topological, and do not necessarily agree with the hyperbolic structure (which, possibly, does not even exist). However, the decomposition corresponds to the straightened ideal polyhedra Π_1, Π_2 in \mathbb{H}^3 in the following way. In Section 2, we described the correspondence between points on the boundary of \mathbb{H}^3 and points on the boundary tori at overpasses/underpasses of L using the diagram labels. This gives the correspondence between the vertices of $\bar{\Pi}_1, \bar{\Pi}_2$ and the vertices of Π_1, Π_2 . By the “straightened” we mean that every arc α of the decomposition of $S^3 - L$, that connects two points on the boundary torus of L (say, points \bar{P}_1 and \bar{P}_2) corresponds to the geodesic γ connecting the corresponding points P_1, P_2 in \mathbb{H}^3 .

Here we will formulate the conditions on the diagram labels that guarantee that the straightened decomposition is properly embedded in \mathbb{H}^3 and can be triangulated so that the conditions (1)-(4) are satisfied.

The sufficient conditions on the diagram labels ensuring the existence of the complete hyperbolic structure are as follows (here and further we assume that the labels satisfy the hyperbolicity equations):

a) Consider labels on two sides of an overpass of a crossing. There are four such labels, $u, v, u+1, v+1$. Let u be the last one as we move in the direction of the link orientation along the overpass strand (Fig.3). Then $\text{Im } u > 0$ holds iff u is on the right with respect to our travel (Fig.3, left), and $\text{Im } u < 0$ holds iff it is on the left (Fig.3, right). This condition only needs to be checked for one arbitrarily chosen edge label of D that is not purely real (if there is such a label).

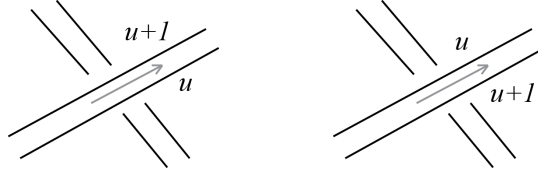


Fig.3

b) For every overpass/underpass that has two consecutive edge labels u, v (Fig.4, left), and is not incident to a bigon, either $\text{Im}(-(v+1)/u) > 0$ and $\text{Im}(-(u+1)/v) > 0$ hold if $\text{Im } u > 0$, or $\text{Im}(-v/(u+1)) > 0$ and $\text{Im}(-u/(v+1)) > 0$ hold if $\text{Im } u < 0$.

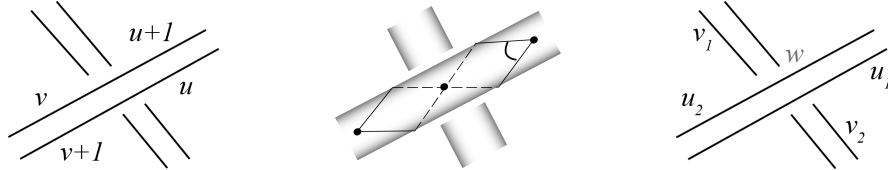


Fig.4

c) There exists a crossing of D for which the following holds. Suppose w is the crossing label assigned to the crossing, and $u_i, i = 1, 2$, are two edge labels on the adjacent overpass, and $v_j, j = 1, 2$ are two edge labels on the adjacent underpass (Fig. 4, right). Then at least one of the fractions $\frac{w}{u_i v_j}, \frac{w}{u_i(v_j+1)}, \frac{w}{v_j(u_i+1)}$ is not purely real for some i, j .

We will now explain the nature of these conditions.

In the polyhedra Π_1, Π_2 , the truncated ideal vertices result in a cross-section that is often a Euclidean quadrilateral. The exception is a cross-section at an ideal vertex that has at least one incident polyhedral edge resulting from a bigon of D . Such a cross-section might be a triangle, or even a bigon that degenerates eventually into just one edge.

Consider a quadrilateral cross-sections of Π_1 . One may see one such cross-sectional tile of the torus boundary on Fig.4, middle, where a crossing of the thickened link is depicted (two of the vertices of the tile are glued together underneath the overpass). The inner Euclidean angles of each quadrilateral correspond to certain dihedral angles of the polyhedron Π_1 .

If we look at the Fig.4, left, we can write the expressions for the angles of the cross-section in terms of the diagram labels. Two opposite angles of the cross-section are $\arg \frac{u}{u+1}$ and $\arg \frac{-v}{-(v+1)}$ (the corresponding quadrilateral is depicted in Fig.5, left). The condition (a) allows to choose the solution to the hyperbolicity equations that is consistent with the orientation conventions used in the definitions of the diagram labels (when choosing out of two Galois conjugates). The consistency for the other labels follows automatically from the equations after the correct choice of the solution is made. Note that if $u = a + bi$ and $\text{Im } u = b > 0$, then $\text{Im} \frac{u}{u+1} = \frac{b}{(a+1)^2 + b^2} > 0$. Therefore, the condition (a) also guarantees that $\text{Im} \frac{u}{u+1}$ and $\text{Im} \frac{v}{v+1}$ are positive, and therefore $\arg \frac{u}{u+1}$ and $\arg \frac{v}{v+1}$ (corresponding to two opposite angles of the quadrilateral cross-section) are between 0 and π . The condition (b) similarly guarantees that two other opposite angles of the cross-section are between 0 and π as well.

In a triangular cross-section of the polyhedron (Fig.5, middle), resulted from collapsing a bigon region of the link diagram, the interior angles correspond to $\arg \frac{u}{u+1}, \arg(u+1), \arg \frac{1}{u}$. Similarly, if $\text{Im } u = b > 0$, then the arguments of $\frac{u}{u+1}, u+1, \frac{1}{u}$ are between 0 and π (since $\text{Im} \frac{1}{u} = b > 0$). Therefore, the conditions (a) and (b) together imply cross-sectional convexity of the Menasco's polyhedra.

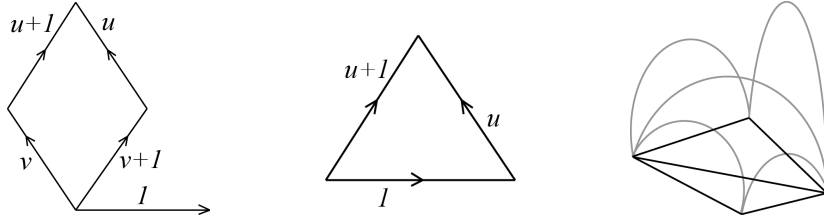


Fig.5

The condition (c) guarantees that we have at least four horospheres that are not all located in the same plane, since the quotient $\frac{w}{u_i v_j}$ is the cross-ratio of the centers of the corresponding horospheres (possibly, with a negative sign). For the details and proof, see Sections 2-4 in [15]. It also ensures that not all crossing labels are 0, which would force the system of hyperbolicity equations to be degenerate, of the form $0 = 0$.

Proposition 4.1. Suppose that for an alternating link L there exists a solution to the hyperbolicity relations such that the conditions (a)–(c) are satisfied. Then each of Π_1, Π_2 is properly embedded in \mathbb{H}^3 , *i.e.* the faces of each polyhedron either are identified, or are disjoint, or

intersect in a connected sequence of edges (including the vertices that are the edges' endpoints), or in an ideal vertex only.

The rest of this section is devoted to the proof of the proposition. The proof consists of a number of observations about the geometric nature of the polyhedra.

Note that it is enough to prove the statement solely for the faces of Π_1 , since the construction of Π_2 is similar to that of Π_1 . Once the Proposition 4.1 holds for any two faces of Π_1 and any two faces of Π_2 , it holds for any pair of faces where one face is from Π_1 and the other face is from Π_2 by the construction as well.

Remove the vertex of Π_1 situated at infinity, and all edges of Π_1 incident to it, and denote the remaining collection of vertices, edges and faces by $\Pi_1 - \{v\}$. In the upper half-space model of \mathbb{H}^3 , let f be the vertical projection of $\Pi_1 - \{v\}$ onto the plane $z = 0$. A fragment of such a projection can be seen on Fig.5, right, with edges of the polyhedron in gray and their image in black.

Lemma 4.2. Under the hypothesis of Proposition 4.1, f is a proper local homeomorphism onto its image.

Proof of Lemma 4.2. Consider two faces $f(K_1), f(K_2)$ of $f(\Pi_1 - \{v\})$ having a sequence of common edges $f_0, f_1, \dots, f_i, i \geq 0$, where each two consecutive edges share a vertex (the proof goes similarly if $f(K_1), f(K_2)$ have only a common vertex). It is enough to show that $f(K_1), f(K_2)$ intersect only in the sequence f_0, f_1, \dots, f_i , i.e. f is a bijection (the rest is obvious by the construction of f).

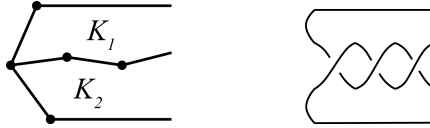


Fig.6

Since K_1, K_2 result from a reduced and twist-reduced alternating diagram, their boundaries can only share a sequence of connected edges (as on Fig.6, left) or a vertex. Indeed, suppose the contrary. Menasco's construction of the polyhedra implies that then there are two faces of D sharing more than a connected sequence of edges or a crossing. In a reduced and twisted-reduced alternating diagram, this is possible only if two adjacent non-bigon regions have a number of bigons between them, as in Fig.6, right, and share several crossings. But the bigons are getting collapsed in Menasco's construction, and result in a row of consecutive edges in the corresponding polyhedra, that the faces share. A contradiction.

Then the same is true for $f(K_1), f(K_2)$ unless the interiors of $f(K_1), f(K_2)$ intersect. By contradiction, suppose now the interiors of $f(K_1), f(K_2)$ intersect.

Since $f(K_1), f(K_2)$ share an edge f_0 , K_1, K_2 share the edge $e_0 = f^{-1}(f_0)$. The interiors of $f(K_1), f(K_2)$ intersect, and therefore one of the other edges of $f(K_1), f(K_2)$ (say, an edge $f(e_1)$ of $f(K_2)$) additionally intersects the interior of the other face ($f(K_1)$). Fig.7, left, demonstrates this for two triangular faces with edges $f(e_0), f(e_1), f(e_2), f(e_3)$. Compare it with Fig.7, right, where the faces with non-intersecting interiors are shown. We will adopt the notations for the edges from this figure. The proof goes similarly if at least one of the faces have more than three sides.

Consider the cross-section Q of Π_1 that corresponds to the ideal vertex incident to e_0, e_1, e_2, e_3 . Denote the vertices of Q by E_0, E_1, E_2, E_3 respectively. The hypothesis of Proposition

4.1 implies that Π_1 is cross-sectionally convex and all interior angles of Q are between 0 and π . Denote the horosphere where Q lies by H . Then, on H , there are two consecutive vertices of Q (say, E_1, E_2) that should be either both above or both below the line passing through the other two vertices. Without loss of generality, suppose E_1, E_2 are above the line E_0E_3 on H . Then in the upper-half space model of \mathbb{H}^3 , the edges e_1, e_2 are represented by longer (in the Euclidean sense) arcs of a circle than e_0, e_3 . Equivalently, for each of e_1, e_2 , the Euclidean distance in the plane $z = 0$ between the two its endpoints is greater than such distance for each of e_0, e_3 .

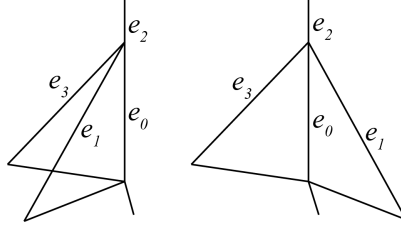


Fig.7

This, together with the assumption that $f(K_1), f(K_2)$ have intersecting interiors, implies that $\Pi_1 - \{v\}$ has at least two layers of faces there, one above another, whose vertices are not at ∞ . We will call them faces of the upper and lower level. We then arrive at one of the four following possibilities for the polyhedron Π_1 .

The first possibility is that one of the faces of the upper level, say, K_3 , is adjacent to a face with a vertex at ∞ or to a face that constitutes the only layer throughout (call this face K_4). We will denote the horosphere adjacent to both K_3, K_4 by H_{34} . This is depicted on Fig.8, left, with the faces of the upper level in black, and the faces of the lower level in grey.

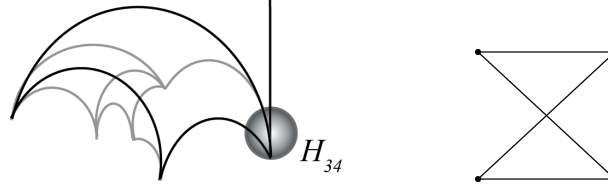


Fig.8

For an edge e of a cross-section Q lying on a horosphere H , the two vertices of Q that are not endpoints of e cannot lie on different sides from the Euclidean line defined by e on H (due to the cross-sectional convexity). However, for the cross-section of $\Pi_1 - \{v\}$ lying on H_{34} this is the case. A contradiction.

A similar argument also guarantees that there is no three or more levels of faces anywhere, which would be the second possibility.

The third possibility is that only the lower level faces are incident to a face (say, K_4) that has a vertex at ∞ . Then, since the boundary of the polyhedron is connected, we arrive at one of the two scenarios. Either K_4 has interior of the polyhedron on both sides near the plane $z = 0$ (as on Fig.9, left). Then on one of the horospheres adjacent to K_4 and not located at ∞ , the cross-section looks like Fig.8, right, again. A contradiction. In the second scenario, none of the faces that are incident to ∞ and to lower level faces simultaneously, have interior of the polyhedron on both sides (as on Fig.9, right). Then the cross-section at the horosphere located at ∞ has angles greater than π (since the exterior angles of the cross-section correspond to the dihedral angles of the polyhedron). A contradiction.

The forth possibility is that the faces of upper and lower levels intersect and exchange levels. This eventually leads us to the possibility number one or two, and the same arguments apply. \square

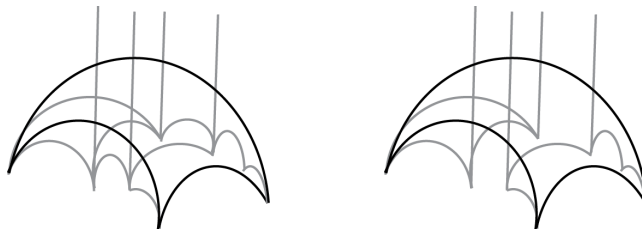


Fig.9

Proof of Proposition 4.1. Being a proper local homeomorphism of two locally compact spaces (open subsets of \mathbb{C}), f is actually a cover. We will then show that f is additionally a homeomorphism.

The proof of Lemma 4.2. implies that for the interior of the faces of $f(\Pi_1 - \{v\})$, the map f is a 1-fold cover. Note also that the vertices and edges of $\Pi_1 - \{v\}$ are sent to the vertices and edges of $f(\Pi_1 - \{v\})$, since f is a vertical projection. So the last thing to check is that f is a 1-fold cover at edges and vertices of $\Pi_1 - \{v\}$, and not a branched cover at any vertex. Suppose the contrary. Then (at least) two ideal vertices v_1, v_2 of $P_1 - \{v\}$ lie at the same point of the plane $z = 0$. This contradicts the condition (c). Therefore, f is a homeomorphism. \square

5 Ideal partially flat geometric triangulations

In this section, we will show that any cross-sectionally convex polyhedra in \mathbb{H}^3 can be subdivided into a partially flat geometric triangulation. This implies that the conditions (a)–(c) guarantee the existence of the complete hyperbolic structure of $S^3 - L$, and the correspondence described in Section 2 induces a developing map.

Theorem 5.1. Suppose that for an alternating link L with the reduced alternating diagram D the edge and crossing labels satisfy the conditions (a)–(c). Then there exists a partially flat geometric triangulation τ that induces the complete hyperbolic structure on $S^3 - L$.

Most of this section is devoted to the proof of the Theorem 5.1.

Under the hypothesis of the theorem, two straightened polyhedra Π_1, Π_2 that correspond to the Menasco's decomposition of $S^3 - L$ are properly embedded in \mathbb{H}^3 by Prop 4.1. First, we construct a triangulation of Π_1, Π_2 that is properly embedded in \mathbb{H}^3 . Recall that f is vertical projection described in the previous section. To begin, subdivide every face F of Π_i into triangles using the existing ideal vertices of F only. Additionally, do it so that for any new edge e subdividing the face F of $\Pi_i, i = 1, 2$, $f(e)$ lies entirely in $f(F)$ (this can always be done as a consequence of the Proposition 4.1). Denote the resulting polyhedra with triangular faces by Π'_i .

Recall that the faces of $\Pi_i, i = 1, 2$, do not have to be planar. Therefore, after we subdivided the faces, we have to check that the resulting polyhedra $\Pi'_i, i = 1, 2$, are properly embedded in \mathbb{H}^3 as well (*i.e.* the new triangular faces do not “cut” through each other). That is the content of the next lemma.

Fix i and consider a cross-section Q' of the polyhedron Π'_i resulted from the subdivision of faces of Π_i as above. Suppose Q' is situated on the horosphere H . Q' corresponds to the 4-sided

cross-section Q of Π_i with the vertices A, B, C, D in the following way: Q' has the four vertices A, B, C, D of Q , and several more vertices resulting from the subdivision of faces of Π_i . We will refer to these vertices as to the “new” vertices of Q' .

Lemma 5.2. Suppose E is new vertex of a cross-section Q' on horosphere H with the center P . Suppose further E resulted from the subdivision of the face of Π_i that is incident to the edge CD of Q . Then either E lies either in the interior of Q , or on CD , or in the part of H bounded by the lines CD, AD, BC and on the other side of the line CD from AB (the area where E may lie is shown on Fig.10.)

Proof of Lemma 5.2. We subdivided the faces of Π_i so that the image of any new edge under f lies entirely in the image of the face it subdivides. Since f is a homeomorphism for Π_i (by Proposition 4.1), any new edge of Π'_i resulting from the subdivision of Π_i does not intersect the interior of any face of Π_i besides the one it subdivides.

Denote the geodesics that pierce H at the points A, B, C, D, E by $\alpha, \beta, \gamma, \delta, \eta$ respectively. If E lies outside the specified area, η pierces a face adjacent to either AD or AB or BC , a contradiction. \square

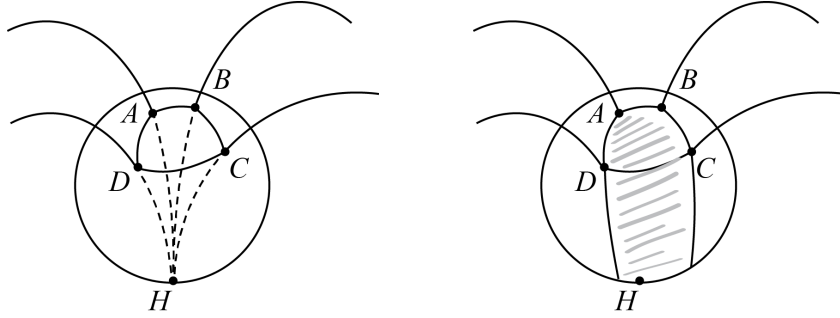


Fig.10

All the faces of Π'_1, Π'_2 are triangular faces, and the previous lemma implies that Π'_1, Π'_2 are properly embedded in \mathbb{H}^3 . We now will construct an ideal partially flat triangulation of Π'_1, Π'_2 , properly embedded in \mathbb{H}^3 .

Triangulate Π'_1, Π'_2 using the existing ideal vertices only, and so that the interiors of the triangular cross-sections of tetrahedra do not intersect. Denote such a triangulation by τ . Note that such τ always exists and is not unique; an example is the triangulation suggested by Thurston and Menasco.

Lemma 5.3. Any tetrahedron in τ is either flat, or lies entirely inside the polyhedron, or lies entirely outside.

Proof of Lemma 5.3. The subdivision of cross-sections of Π'_i corresponds to the subdivision of the polyhedron Π'_i in the following way. Suppose, we subdivided the cross-section Q' with the consecutive vertices A, B, C, D, E on the horosphere H by a new edge EC . Suppose P is the center of H . Suppose also that the vertices A, B, C, D, E result from geodesics $\alpha, \beta, \gamma, \delta, \eta$ respectively (as before) piercing H , and that these geodesics are edges of Π'_i . Then the plane P_{EC} defined by the geodesics γ, η intersects Q' in EC . Suppose also that P_1, P_2 are the ideal vertices that are adjacent to γ, η respectively on the sides opposite of P . We subdivide the cross-section Q' of Π'_i by an edge EC if we also subdivide Π'_i by a new triangular face that lies in the plane P_{EC} and has vertices P, P_1, P_2 (possibly with a new edge between P_1 and P_2).

After the triangulation process, all cross-sections of Π'_i are subdivided into triangles. If there is a tetrahedron T of τ that lies partially outside and partially in the polyhedron Π'_i in \mathbb{H}^3 , then at least one of the faces (say, a face F) of T is partially outside and partially in Π'_i . Then in the corresponding cross-section we have a subdividing edge that is partially inside and partially outside it, *i.e.* the edges of the cross-section intersect more than just in their endpoints. This is not possible by Lemma 5.2, and by our construction of the triangulation. Similar argument shows that the interior of any truncated tetrahedron is not intersected by another truncated tetrahedron. \square

Proof of Theorem 5.1. Lemma 5.3 implies that τ is an ideal partially flat triangulation, and the condition (3) from Section 3 is satisfied. Now let us check the conditions (1), (2) and (4).

We start with (4). Recall that every overpass or underpass of the diagram D corresponds to an ideal vertex of Π_i , and, therefore, of the triangulation τ in \mathbb{H}^3 . Every edge connecting the vertices v_i and v_j of τ lies on a geodesic that connects the centers of the corresponding horospheres (denote them by H_i, H_j). Hence, a quadrilateral cross-section of Π_i results from connecting one of the horospheres with four neighboring horospheres by four distinct arcs (Fig.11, left, shows this for a horosphere H_1). Since u_1, u_2, u_3, u_4 satisfy the definition of the edge labels, they are determined by the Euclidean translations between the points where the four intercusp arcs pierce H_1 . This implies that the picture that corresponds to a cross-section of a polyhedron Π_i is complete.

We then triangulated the polyhedra Π_1, Π_2 by adding more arcs (edges) between the existing ideal vertices. For an ideal vertex v_1 , all the arcs of the triangulation start at H_1 and end at one of the neighboring horospheres, that correspond to other overpasses and underpasses. For a new arc γ , define u'_3 and u''_3 be the translations between the point where γ pierces H_1 , and the points where the arcs next to the right and next to the left to γ pierce H_1 . These translations can be found from the previous labels using the edge and region relations, which imply completeness. In particular, $u'_3 + u''_3 = u_3$ (Fig.11, right).

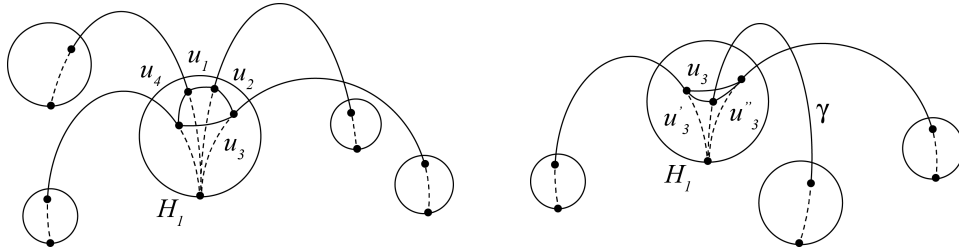


Fig.11

Let us now look at the condition (2). Choose an edge e of τ , and let T_1, \dots, T_k be tetrahedra glued at e . Their shapes are the ratios of the edge labels $z_1 = u_1/u_2, z_2 = u_2/u_3, \dots, z_{k-1} = u_{k-1}/u_k, z_k = u_k/u_1$, where each u_i connects the point where e pierces H_1 with the points where other edges of T_1, T_2, \dots, T_k pierce H_1 (Fig.12, left). None of u_i is 0 due to the conditions (a)-(c), and the product of such shapes then satisfies $z_1 \dots z_k = 1$.

Turn our attention to the condition (1). Consider a tetrahedron T in the triangulation τ . Suppose the (complex) translations corresponding to the sides of a cross-section lying at the horosphere H_1 are $u_1, v_1, -(u_1 + v_1)$. Let the geodesics of T be denoted by $\gamma_i, i = 1, 2, \dots, 5$ as on Fig.12, right. Then the shapes associated with the geodesics γ_1, γ_2 and γ_3 are $-\frac{v_1}{u_1}$,

$\frac{u_1}{u_1 + v_1}$, $\frac{u + v}{v}$. Denote the first shape by z , and then the other two shapes are $1 - \frac{1}{z}$, $\frac{1}{1 - z}$. The corresponding Euclidean angles of the cross-section are arguments of the shapes, and so are three corresponding dihedral angles.

We need to check whether the opposite dihedral angles in T agree. For this, it is enough to check that the shapes agree. Suppose, another cross-section of T lying on the horosphere H_2 has sides $u_2, v_2, -(u_2 + v_2)$.

Diagram labels satisfy the region relations, and the relations are obtained by composing the isometries rotating (truncated) hyperbolic polygons. The polygons are preimages of the boundary of regions of D . We may use faces of a triangulation instead of the regions (the labels are defined so that they satisfy the relations coming from rotating these faces as well). All these faces are three-sided, which makes the relations particularly simple.

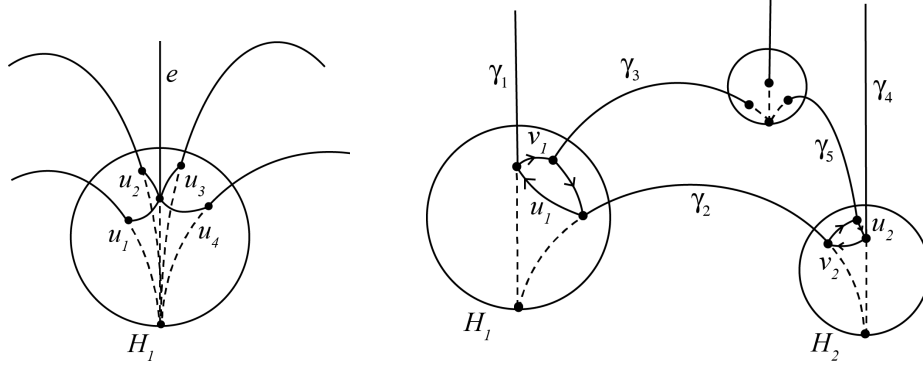


Fig.12

Let us show that the shape of T associated with γ_3 is equal to the shape of T associated with γ_4 . The former is $\frac{u_1 + v_1}{v_1}$, while the latter is $\frac{-v_2}{u_2}$.

From the 3-sided polygon, that is a face of T , determined by geodesics $\gamma_1, \gamma_2, \gamma_4$: $\frac{w_2}{u_1 v_1} = 1$, and therefore $v_2 = \frac{w_2}{u_1}$. From the 3-sided polygon, that is a face of T , determined by $\gamma_3, \gamma_2, \gamma_5$: $\frac{w_2}{(u_1 + v_1)(u_2 + v_2)} = 1$, and therefore $u_2 + v_2 = \frac{w_2}{u_1 + v_1}$. Then, from the cross-section of T on the horosphere H_2 , $u_2 = (u_2 + v_2) - v_2 = \frac{w_2}{u_1 + v_1} - \frac{w_2}{u_1}$.

Substitute the above expressions for v_2 and u_2 in the shape of T associated with γ_4 . After routine simplifications, we obtain $\frac{-v_2}{u_2} = -\frac{u_1 + v_1}{v_1}$, which is exactly the shape of T associated with γ_3 . Similarly one can show that other pairs of shapes of T agree.

Note also that the condition (c) implies that not all tetrahedra have 0 volume, since there are at least four ideal vertices not all lying in one plane (as explained in Section 4).

Since the conditions (1)-(4) are satisfied by τ , we may use Theorem 1.1 from [12] to state that the complete hyperbolic structure on $S^3 - L$ exists. \square

The next statement follows from our construction.

Corollary 5.4. Once a hyperbolic 3-manifold M has a decomposition into two ideal cross-sectionally convex polyhedra in \mathbb{H}^3 , there exists an ideal partially flat geometric triangulation of M .

6 Isotopy classes of crossing arcs

The following statement provides a method to determine isotopy classes of crossing arcs. Note that to check the conditions (a)-(c), one does not have to perform a triangulation.

Proposition 6.1. Under the conditions (a)-(c) on the diagram labels of a reduced alternating diagram D of a link L , its crossing arcs are isotopic to simple geodesics.

Proof. The proof of Theorem 1.1. from [12] implies that the topological space obtained by gluing the tetrahedra (some, possibly, flat) is homeomorphic to $S^3 - L$, and that the hyperbolic structure of $S^3 - L$ locally induces its own metric on each tetrahedron. Therefore, the edges of τ are geodesics in \mathbb{H}^3 , and the tetrahedra of τ are isometric to the corresponding tetrahedra in $S^3 - L$, making the edges of the corresponding triangulation of $S^3 - L$ geodesics as well. By Thurston-Menasco's construction of the polyhedra (that we later triangulated, obtaining τ), every crossing arc of D is an edge of τ .

Let us now check that the crossing arcs are simple geodesics, *i.e.* have no self-intersections. The only edges of τ that intersect in one point in \mathbb{H}^3 are two distinct edges of a flat tetrahedron (and, respectively, the edges that are identified with these two edges under the gluing). We need to check that these edges do not correspond to the same crossing arc in $S^3 - L$. By the Thurston-Menasco's construction, a crossing arc c in $S^3 - L$ corresponds to one edge e_1 of Π_1 , and one edge e_2 of Π_2 . Under the gluing, e_1 and e_2 are identified, and therefore they cannot be two distinct edges of one geometric tetrahedron intersecting in just one point. \square

The following examples illustrate that the conditions (a)-(c) are not too restrictive, and also show how to check them in practice. The first example is an infinite family of alternating braids, and the second one is an alternating link randomly chosen from the tables. To my knowledge, nothing was known about isotopy classes of their crossing arcs before. Empirical data suggests that many other hyperbolic alternating links satisfy the conditions (a)-(c).

Example 6.2. Consider an infinite family of alternating closed braids $(\sigma_1\sigma_3\sigma_2^{-1})^n$ and $(\sigma_1\sigma_3\sigma_2^{-1})^n\sigma_1\sigma_3$, $n > 1$. Fig.13, left, shows a fragment of such link with the diagram labels. The link can always be oriented as on the figure. Then the symmetry together with the relations for 3-sided region imply that there is only one edge label, u_1 , and all the crossing labels are $\pm w_1$, where the sign depends on whether we the crossing is negative (as the crossings in the middle on Fig.13, left) or positive (as the leftmost and rightmost crossings on Fig.13, left).

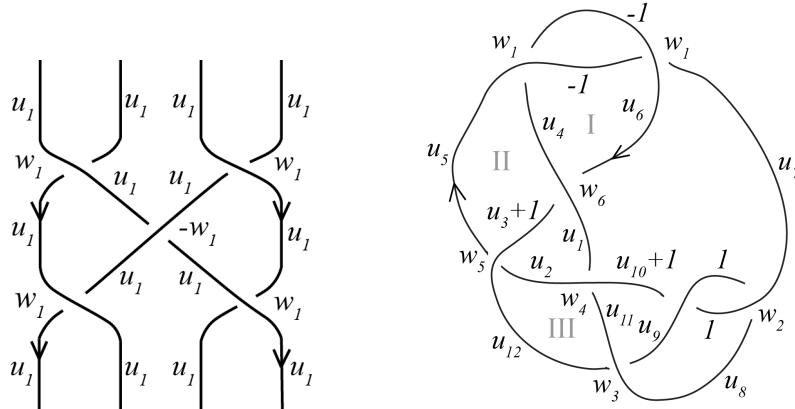


Fig.13

The shape (in the sense of [15]) of the regular n -sided region was established in [15] and is $\frac{w_1}{u_1^2} = \left(\frac{1}{2} \sec \frac{\pi}{n}\right)^2$. Then the labels that satisfy the conditions (a)-(c) are $w_1 = i/2, u_1 = (-1 - i)/2$.

The same argument applies to any alternating closed braid of the type either $(\sigma_1\sigma_3\ldots\sigma_{2k+1}\sigma_2\sigma_4\ldots\sigma_{2k}^{-1})^n$ or $(\sigma_1\sigma_3\ldots\sigma_{2k+1}\sigma_2^{-1}\ldots\sigma_{2k}^{-1})^n\sigma_1\sigma_3, n > 1$, showing that the crossing arcs of the reduced alternating diagram of such a link are isotopic to geodesics. Note that these are braids that have an even index. One may also use similar argument for closed alternating braids with no bigons of odd index, generalizing Example 6.2 from [15].

Example 6.3. Consider the 2-component link 8_8^2 in the Rolfsen table, and its reduced alternating diagram (Fig.13, right). Assign diagram labels and orientation to it as on the figure. Recall that every region yields three region relations. Below we give the relations, and the decimal values of the labels necessary to check the conditions (a)-(c). This simple calculation shows that all the crossing arcs are isotopic to geodesics.

From the regions I, II, III respectively: $w_1 + u_6 = 0, w_6 - u_6u_4 = 0, w_1 + u_4 = 0, w_1 + (u_4 + 1)(u_5 + 1) = 0, w_5 - (u_5 + 1)(u_3 + 1) = 0, w_6 + (u_4 + 1)(u_3 + 1) = 0, w_5 - (u_{12} + 1)(u_2 + 1) = 0, w_4 - (u_2 + 1)(u_{11} + 1) = 0, w_3 - (u_{11} + 1)(u_{12} + 1) = 0$.

From the other three 3-sided regions: $w_6 - u_3u_1 = 0, w_4 + u_2u_1 = 0, w_5 + u_2u_3 = 0, w_2 - u_{10}u_9 = 0, w_3 + u_{11}u_9 = 0, w_4 + u_{10}u_{11} = 0, w_2 + u_8 + 1 = 0, w_3 - (u_8 + 1)(u_9 + 1) = 0, w_2 + u_9 + 1 = 0$.

Lastly, of the two 5-sided regions (one of which is the outer region of the diagram), each yields equations of the form $\xi_1\xi_3 - (\xi_1 + \xi_2 + \xi_3) + 1 = 0, \xi_2\xi_4 - (\xi_2 + \xi_3 + \xi_4) + 1 = 0, \xi_3\xi_5 - (\xi_3 + \xi_4 + \xi_5) + 1 = 0$, where for the inner region $\xi_1 = \frac{-w_1}{(u_6 + 1)(u_7 + 1)}, \xi_2 = \frac{-w_2}{u_7 + 1}, \xi_3 = \frac{-w_2}{u_{10} + 1}, \xi_4 = \frac{w_4}{(u_1 + 1)(u_{10} + 1)}, \xi_5 = \frac{-w_6}{(u_1 + 1)(u_6 + 1)}$, and for the outer $\xi_1 = \frac{-w_1}{u_7}, \xi_2 = \frac{w_2}{u_7u_8}, \xi_3 = \frac{-w_3}{u_{12}u_8}, \xi_4 = \frac{-w_5}{u_{12}u_5}, \xi_5 = \frac{w_1}{-u_5}$.

One can then use a computer algebra system to obtain the solutions. The solution that satisfies the condition (a)-(c) has the following approximate decimal values of the labels: $w_1 = 0.37 - 0.52i, w_2 = -0.37 - 0.52i, w_3 = -0.13 + 0.39i, w_4 = 0.19 + 0.34i, w_5 = -0.19 + 0.34i, w_6 = -0.13 - 0.39i, u_1 = -0.08 + 0.63i, u_2 = -0.5 + 0.36i, u_3 = -0.58 + 0.27i, u_4 = u_6 = -0.37 + 0.52i, u_5 = -0.85 + 0.78i, u_7 = -0.5 + 1.9i, u_8 = u_9 = -0.63 + 0.52i, u_{10} = -0.05 + 0.78i, u_{11} = -0.42 + 0.27i, u_{12} = -0.92 + 0.63i$. Therefore, the crossing arcs of the diagram on Fig.13, right, are isotopic to geodesics.

7 Acknowledgments

I am grateful to Marc Lackenby for many enlightening conversations and for being a host for my visits to the University of Oxford where this research was started; to Marc Culler, Carlo Petronio, and Jessica Purcell for helpful comments and correspondence; to Joel Hass and Abigail Thompson for interest in this work and encouragement. The work was partially supported by the NSF-AWM travel mentoring grant, and by the NSF DMS-1406588 grant.

References

- [1] Colin C. Adams, *Unknotting tunnels in hyperbolic 3-manifolds*, Math. Ann. 302 (1995), no. 1, 177–195.
- [2] Colin C. Adams, Alan W. Reid, *Unknotting tunnels in two-bridge knot and link complements*, Comment. Math. Helv. 71 (1996), no. 4, 617–627.
- [3] S. D. Burton, J. S. Purcell, *Geodesic systems of tunnels in hyperbolic 3-manifolds*, Algebr. Geom. Topol. 14 (2014), no. 2, 925–952.
- [4] D. Cooper, D. Futer, J. Purcell, *Dehn filling and the geometry of unknotting tunnels*, Geom. Topol., Vol. 17 (2013), no. 3, 1815–1876.
- [5] M. Lackenby, *The volume of hyperbolic alternating link complements*, with an appendix by I. Agol and D. Thurston., Proc. London Math. Soc. (3) 88 (2004), no. 1, 204–224.
- [6] M. Lackenby, *An algorithm to determine the Heegaard genus of simple 3-manifolds with nonempty boundary*, Algebr. Geom. Topol. 8 (2008) 911–934.
- [7] W. W. Menasco, *Polyhedra representation of link complements*, Low-dimensional topology (San Francisco, Calif., 1981), 305–325, Contemp. Math., 20, Amer. Math. Soc., Providence, RI, 1983.
- [8] S. M. Miller, *Geodesic knots in the figure-eight knot complement*, Experiment. Math. 10 (2001), no. 3, 419–436.
- [9] D. Mostow, *Quasi-conformal mappings in n -space and the rigidity of the hyperbolic space forms*, Publ. Math. IHES 34 (1968), 53–104.
- [10] G. Prasad, *Strong rigidity of Q -rank 1 lattices*, Invent. Math. 21 (1973), 255–286.
- [11] C. Petronio, *An algorithm producing hyperbolicity equations for a link complement in S^3* , Geom. Dedicata 44 (1992), no. 1, 67–104.
- [12] C. Petronio, J. R. Weeks, *Partially flat ideal triangulations of cusped hyperbolic 3-manifolds*, Osaka J. Math. 37 (2000), 453–466.
- [13] M. Sakuma and J. R. Weeks, *Examples of canonical decomposition of hyperbolic link complements*, Japan. J. Math. (N. S.) 21 (1995), No. 2, 393–439.
- [14] W. P. Thurston, *The geometry and Topology of Three-Manifolds*, Electronic Version 1.1 (March 2002), <http://www.msri.org/publications/books/gt3m/>
- [15] M. Thistlethwaite, A. Tsvietkova, *An alternative approach to hyperbolic structures on link complements*, Algebr. Geom. Topol. 14 (2014), 1307–1337.
- [16] J. R. Weeks, *SnapPea: a computer program for creating and studying hyperbolic 3-manifolds*, freely available from <http://thames.northnet.org/weeks/index/SnapPea.html>

Anastasiia Tsvietkova
Department of Mathematics
University of California, Davis
One Shields Ave, Davis, CA 95616, USA
tsvietkova@math.ucdavis.edu